

# Non-Isothermal Crystallization and Thermal Degradation Kinetics of Biodegradable Poly(butylene adipate-co-terephthalate)/Starch Blends

Surasak Chiangga<sup>1,\*</sup>, Satayu Suwannasopon<sup>2</sup>  
and Nutnarun (Supreya) Trivijitkasem<sup>1</sup>

## ABSTRACT

The non-isothermal crystallization behavior of biodegradable poly (butylene adipate-co-terephthalate)/starch (PBAT/S) blends was studied using differential scanning calorimetry under a nitrogen atmosphere from 25 to 225 °C at four constant cooling rates of 5, 10, 15 and 20 °C·min<sup>-1</sup>. There was only one crystallization peak in the exothermic curve which shifted to a lower temperature as the cooling rate was increased. The crystallization temperature decreased from 98 to 84 °C, but the crystallization enthalpy increased from 11 to 12 J·g<sup>-1</sup> as the heating rate was increased.

The thermal degradation(TG) of the PBAT/S blends was studied using thermogravimetric analysis under a nitrogen atmosphere from 100 to 800 °C at five constant heating rates of 1, 2, 5, 10, and 15 °C·min<sup>-1</sup>. The TG curves showed two degradation stages occurring at 309–342 °C and 375–420 °C, which were the degradation of corn starch and PBAT, respectively.

The thermal degradation kinetics of the PBAT/S were analyzed using the isoconversion Flynn-Wall-Ozawa model-free method. The results showed that both the apparent activation energy and the logarithm pre-exponent factor increased with increasing conversion  $\alpha$ . The average apparent activation energy and the average logarithm apparent pre-exponent factor for  $\alpha = 0.1 - 0.9$  were 266 kJ·mol<sup>-1</sup> and 37 min<sup>-1</sup>, respectively. The reaction model  $g(\alpha)$  determined from the master plot method for PBAT/S was a phase-boundary controlled reaction, where  $g(\alpha) = [1 - (1 - \alpha)^{1/2}]$  .

**Keywords:** PBAT/S, non-isothermal crystallization, thermal degradation kinetics, reaction model

## INTRODUCTION

Polymeric materials are used in large quantities for packaging and industrial applications, which has caused a rapid increase in the amount of plastic waste. Recycling and the reuse of non-degradable polymeric materials are suitable options from an ecological and an economic perspective. An alternative way is to develop blends of polymer (Ge *et al.*, 2005; Girija *et al.*, 2005).

Up to now, biodegradable polymeric materials and composites have been developed from both petrochemical-based feedstock and from renewable resources to replace the conventional plastics in the interests of environmental protection; they exhibit satisfactory thermal and mechanical properties (Jun, 2000; Chrissafis *et al.*, 2006).

Poly(butylene adipate-co-terephthalate) (PBAT), is an aliphatic-aromatic biodegradable polymer, which is synthesized from petrochemical-based

<sup>1</sup> Department of Physics, Faculty of Science, Kasetsart University, Bangkok 10900, Thailand.

<sup>2</sup> Department of Physics, Faculty of Science, Siam University, Bangkok 10160, Thailand.

\* Corresponding author, e-mail:fscissc@ku.ac.th

feedstock. It shows properties similar to low-density polyethylene which is not biodegradable, but there are some properties that prevent the use of PBAT for extensive applications in the market, such as its high price and its thermal degradability temperature which is slightly higher than its melting point (Vromana and Tighzert, 2009; Sugish, 2008 and Mohanty and Nayak, 2010).

In this work, corn starch, an inexpensive naturally occurring degradable polymer, was blended with PBAT to induce thermal stability and reduce the cost of the product.

Characterizing the non-isothermal crystallization and thermal degradation kinetics of biodegradable poly (butylene adipate-co-terephthalate)/corn starch (PBAT/S) blends provides important information about the physical transition and thermal degradation mechanism and non-isothermal crystallization, respectively. The technique used for studying thermal properties is differential scanning calorimetry (DSC). Thermogravimetric analysis (TGA) provides valuable information for evaluating thermogravimetric kinetic parameters. The isoconversion model-free methods are used to determine reliable kinetic information from both isothermal and non-isothermal conditions (Sanchez *et al.*, 2009; Vyazovkin and Wight, 1999). Here, the isoconversion Flynn-Wall-Ozawa (FWO) model-free method was used to analyze thermal degradation kinetic parameters, and the reaction model was investigated using the master plot method.

## MATERIALS AND METHODS

PBAT/S blends were supplied from Thantawan Industry PLC., Nakhon Pathom, Thailand. Differential scanning calorimetry (DSC) experiments were carried out using a differential scanning calorimeter (DSC 7; Perkin-Elmer; Waltham, MA, USA). The temperature and heat flow were calibrated with an indium standard under

the same conditions for all samples. All samples were sealed in aluminum pans. The analyses were performed on 7–10 mg samples from 25 to 225 °C at four heating rates of 5, 10, 15 and 20 °C·min<sup>-1</sup>. A nitrogen atmosphere with a constant flow rate of 20 mL·min<sup>-1</sup> was applied. The melting temperature ( $T_m$ ) was measured from the endothermic curve. Afterward, the samples were maintained at 225 °C for 5 min to erase the previous thermal history, followed by non-isothermal crystallization being performed at four cooling rates of 5, 10, 15 and 20 °C·min<sup>-1</sup>. The crystallization temperature ( $T_c$ ) was measured from the exothermic curve, and the crystallization enthalpy ( $\Delta H_c$ ) was determined from the area under the exothermic peak.

TGA experiments were carried out using thermogravimetric analysis (TGA7; Perkin-Elmer; Perkin-Elmer; Waltham, MA, USA) under a nitrogen atmosphere with a constant flow rate of 20 mL·min<sup>-1</sup>. Each sample (thickness 44 μm, weight 1.3 ± 0.2 mg) was placed in a platinum pan. Non-isothermal experiments were performed from 100–800 °C at five heating rates of 1, 2, 5, 10, and 15 °C·min<sup>-1</sup>.

## RESULTS AND DISCUSSION

### Crystallization behavior

The non-isothermal DSC thermograms for the PBAT/S blends were recorded as a function of temperature ( $T$ ) at four heating and four cooling rates. The DSC cooling curves are presented in Figure 1a which show only one exothermic peak of the non-isothermal crystallization which shifts to a lower temperature at a higher cooling rate. The melting temperatures are reported in Table 1 and show an increase with an increasing heating rate.

The crystallization temperature and crystallization enthalpy results are also reported in Table 1;  $T_c$  decreases, but  $\Delta H_c$  increases as the cooling rate increases.

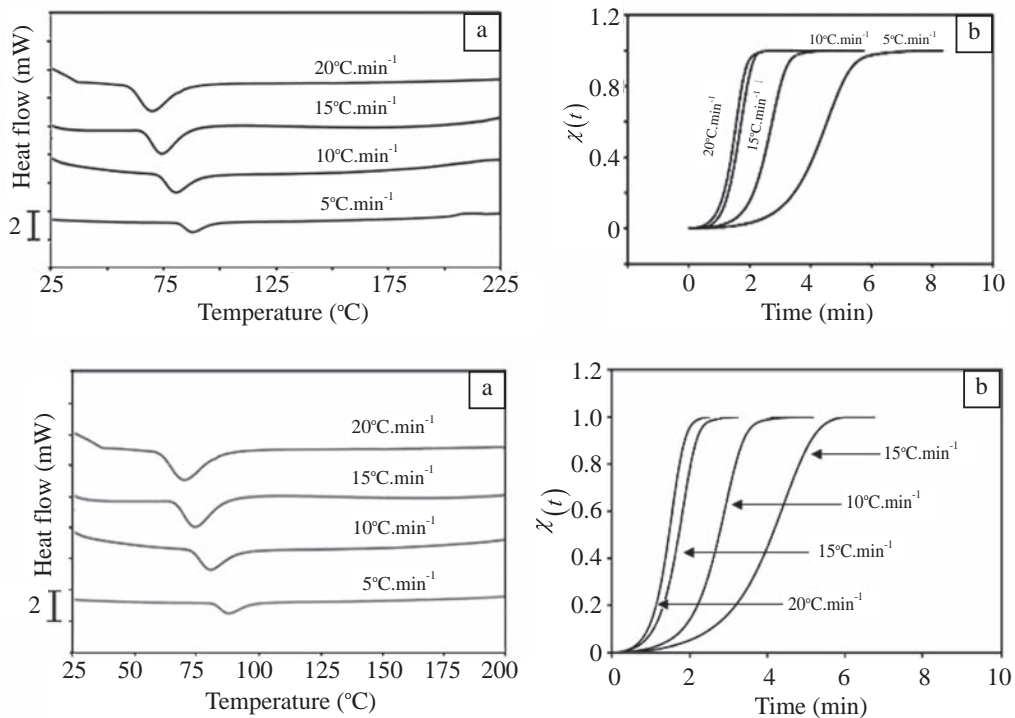


**Figure 1** (a) Differential scanning calorimetry thermograms; and (b) Relative crystallinity  $\chi_{(t)}$  of the non-isothermal crystallization at four cooling rates for poly (butylene adipate-co-terephthalate)/starch blends.

**Table 1** Melting temperature ( $T_m$ ), crystallization temperature ( $T_c$ ), and crystallization Enthalpy ( $\Delta H_c$ ) at rate of changing temperature ( $\varphi$ ) for poly (butylene adipate-co-terephthalate)/starch blends.

$\varphi$ (°C·min⁻¹)	$T_m$ (°C)	$T_c$ (°C)	$\Delta H_c$ (J·g⁻¹)	$\tau_{1/2}$ (min)
5	141.9	97.9	10.8	4.3
10	140.6	91.7	11.3	2.6
15	140.2	86.4	11.7	1.6
20	140.0	83.6	12.0	1.5

The relative crystallinity  $\chi(T)$  at temperature  $T$  can be determined from Equation 1:

$$\chi(T) = \frac{\Delta H_c}{\Delta H_\infty} \quad (1)$$

where  $\Delta H_c$  is the total enthalpy released during crystallization at temperature  $T$  and  $\Delta H_\infty$  is the complete crystallization enthalpy.

The relative crystallinity  $\chi(t)$  at time  $t$  can be determined conversely from the relative

crystallinity  $\chi(t)$  at temperature  $T$  using Equation 2:

$$t = (T_0 - T) / \varphi \quad (2)$$

where  $T_0$  is the initial crystallization temperature and  $\varphi$  is the cooling rate.

The relative crystallinity as a function of time determined from the  $\chi(T)$  curve and Equation 2, as described by Trivijitkasem *et al.* (2008), is presented in Figure 1b. The non-isothermal

crystallization half time ( $\tau_{1/2}$ ) determined from Figure 1b is reported in Table 1, which shows a longer crystallization half time at a lower cooling rate.

### Thermogravimetric measurement

Thermal degradation of the PBAT/S blends recorded as a function of temperature at five heating rates is shown in Figure 2a. The TG curve shifts to a higher temperature at a higher heating rate. There were two weight loss stages: the first one appeared at a lower temperature between 309 and 342 °C and represented the degradation of corn starch, while the second one at a higher temperature between 375 and 420 °C showed the degradation of PBAT (Mano *et al.*, 2003; Mohanty and Nayak, 2010).

The conversion  $\alpha$  can be determined from the weight loss TG curves using the following equation:

$$\alpha = \frac{w_0 - w}{w_0 - w_\infty} \quad (3)$$

where  $w_0$ ,  $w$  and  $w_\infty$  are the initial weight, the actual weight at temperature  $T$  and the final weight of the degradation process, respectively.

The derivative weight loss  $da/dT$  curves or DTG curves shown in Figure 2b were determined from the TG curves. There were two peaks for each heating rate.

The two peak temperatures, the final complete degradation temperature and the degradation content for corn starch, PBAT and ash obtained from the TG and DTG curves at various heating rates are reported in Table 2. The three characteristic temperatures increased with an increased heating rate.

### Thermal degradation kinetics

The thermal degradation kinetics for the non-isothermal process can be analyzed from various methods. Here the isoconversion Flynn-Wall-Ozawa (FWO) model-free method was used as shown in Equation 4 (Chiangga *et al.*, 2012):

$$\ln \beta = \ln \left( \frac{A_\alpha E_\alpha}{R g(\alpha)} \right) - 5.331 - 1.052 \frac{E_\alpha}{RT} \quad (4)$$

where  $\beta$  is the heating rate,  $A_\alpha$  is the apparent pre-exponent factor,  $E_\alpha$  is the apparent activation energy,  $R$  is the gas constant ( $8.3136 \text{ J.mol}^{-1} \text{ K}^{-1}$ ),  $g(\alpha)$  is the integral form of the reaction model and  $T$  is the temperature.

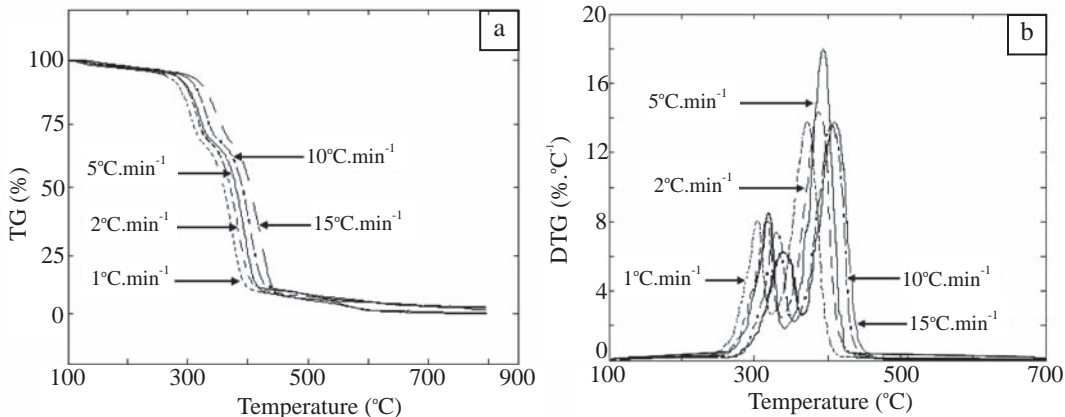


**Figure 2** (a) Thermal degradation (TG); and (b) Derivative weight loss (DTG) curves for poly (butylene adipate-co-terephthalate)/starch blends.

**Table 2** Characteristic temperatures for peak 1 ( $T_{p1}$ ) and peak 2 ( $T_{p2}$ ) and the degradation content for corn starch (S), poly (butylene adipate-co-terephthalate)/starch blends(PBAT) and ash (A) at different heating rates( $\beta$ ).

$\beta$ ( $^{\circ}\text{C} \cdot \text{min}^{-1}$ )	$T_{p1}$ ( $^{\circ}\text{C}$ )	$T_{p2}$ ( $^{\circ}\text{C}$ )	$T_f$ ( $^{\circ}\text{C}$ )	S (%)	PBAT (%)	A (%)
1	309	375	428	25.7	72.2	0.9
2	318	387	460	24.0	74.1	0.9
5	320	398	489	24.6	72.9	0.8
10	333	417	501	25.4	72.6	0.9
15	342	420	527	27.2	70.0	0.8

According to Equation 4, plotting  $\ln \beta$  versus  $1/T$ , using the data obtained from the TG curves for the different heating rates ( $\beta$ ) and fixed values of  $\alpha$ , provides a straight line. The slope ( $-1.052 E_\alpha / R$ ), can be used for evaluating the apparent activation energy and the intercept ( $\ln[A_\alpha E_\alpha / Rg(\alpha)]$ ) can be used for evaluating the logarithm apparent pre-exponent factor ( $\ln A_\alpha$ ).

The FWO plots for PBAT/S for the conversion values  $\alpha = 0.1, 0.2, \dots, 0.9$  are shown in Figure 3. The linear correlation was greater than 0.99. The apparent activation energy and the linear correlation coefficient for each conversion  $\alpha$  value were determined from the slope and the deviation of the lines, respectively, and are reported in Table 3.

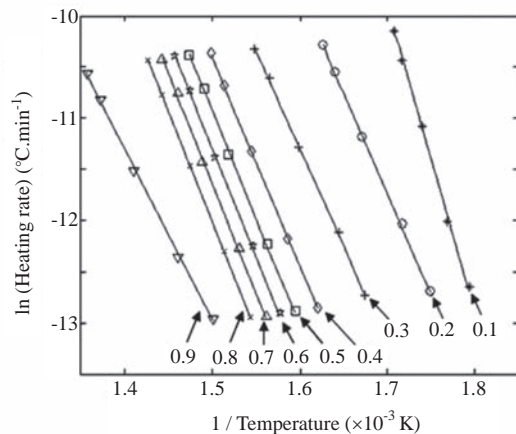


**Figure 3** Plots of natural logarithm of the heating rate ( $\beta$ ) versus the reciprocal of temperature ( $T^{-1}$ ) for poly (butylene adipate-co-terephthalate)/starch blends.

**Table 3** Apparent activation energy ( $E_\alpha$ ) and logarithm apparent pre-exponent factor ( $\ln A_\alpha$ ) for poly (butylene adipate-co-terephthalate)/starch blends at different values of conversion ( $\alpha$ ).

$\alpha$	$E_\alpha$ ( $\text{kJ} \cdot \text{mol}^{-1}$ )	$\ln A_\alpha$ ( $\text{min}^{-1}$ )
0.1	214.4	30.63
0.2	261.2	36.10
0.3	262.6	36.75
0.4	269.6	36.82
0.5	275.6	38.43
0.6	276.3	38.55
0.7	277.4	38.80
0.8	278.1	38.93
0.9	280.0	39.05
Mean	266.1	37.12

The variation of the apparent activation energy ( $E_a$ ) as a function of conversion  $\alpha$  for the PBAT/S blends is shown in Figure 4.  $E_a$  increased as the conversion  $\alpha$  was increased. The apparent activation energy was 214 kJ.mol<sup>-1</sup> at  $\alpha = 0.1$  and increased rapidly to 261 kJ.mol<sup>-1</sup> at  $\alpha = 0.2$ , then increased slowly to 280 kJ.mol<sup>-1</sup> at  $\alpha = 0.9$ . The increase in  $E_a$  with conversion  $\alpha$  implies a multi-step degradation mechanism of the PBAT/S blends. The average apparent activation energy was 266 kJ.mol<sup>-1</sup>. A greater activation energy indicates higher thermal stability.

### Determination of reaction model

The integral form of the reaction model  $g(\alpha)$  is defined in Equation 5 (Jankovic *et al.*, 2007):

$$g(\alpha) = \int_0^{\alpha} \frac{d\alpha}{f(\alpha)} = \frac{A}{\beta} \int_{T_0}^T \exp\left(\frac{-E_a}{RT}\right) dT \quad (5)$$

where  $f(\alpha)$  is the differential form of reaction model and  $T_0$  is the initial temperature. Equation 5 can be transformed into Equation 6 using  $x = E_a/RT$  and Equation 7:

$$g(\alpha) = \frac{AE_a}{R\beta} \int_x^{\infty} \frac{\exp(-x)}{x^2} dx = \frac{AE_a}{R\beta} p(x) \quad (6)$$

$$\text{where } p(x) = \int_x^{\infty} \frac{\exp(-x)}{x^2} dx \quad (7)$$

At a reference point,  $\alpha = 0.5$ , Equation 6 is then modified to Equation 8:

$$g(0.5) = \frac{AE_a}{R\beta} p(x_{0.5}) \quad (8)$$

where  $x_{0.5} = E_a/RT_{0.5}$  and  $T_{0.5}$  is the temperature at conversion  $\alpha = 0.5$ .

Dividing Equation 6 by Equation 8, produces Equation 9:

$$\frac{g(\alpha)}{g(0.5)} = \frac{p(x)}{p(x_{0.5})} \quad (9)$$

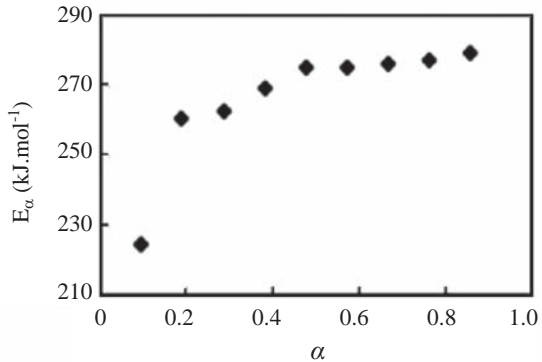


**Figure 4** Dependence of the apparent activation energy ( $E_a$ ) on conversion  $\alpha$  for poly(butylene adipate-co-terephthalate)/starch blends.

There is no analytical solution for  $p(x)$ , so the approximate formula for  $p(x)$  with high accuracy was used as shown in Equation 10:

$$p(x) = \frac{\exp(-x)}{x} \cdot \left( \frac{x^3 + 18x^2 + 86x + 96}{x^4 + 20x^3 + 120x^2 + 240x + 120} \right) \quad (10)$$

The values of  $p(x)$  and  $p(x_{0.5})$  can be calculated from Equation 10 using the experimental data of  $E_a$  from Figure 3 at different heating rates of  $\beta$ .

Utilizing the master-plot method, the reaction model  $g(\alpha)$  can be investigated (Ramis *et al.*, 2004; Saha and Ghoshal, 2007). Figure 5 shows the theoretical master plots of various  $g(\alpha)/(0.5)$  functions versus  $\alpha$ : 1) phase-boundary controlled reaction (contracting area), R2; 2) two-dimensional diffusion (bidimensional particle shape), D2; 3) Avrami-Erofeev ( $m = 2$ ), A2; 4) Avrami-Erofeev ( $m = 3$ ), A3; 5) first-order (Mampel), F1; and 6) power 3, P3. The experimental master plots of  $p(x)/p(x_{0.5})$  versus  $\alpha$  are also shown in Figure 5.

For a given conversion  $\alpha$ , the experimental values of  $p(x)/p(x_{0.5})$  and theoretically calculated values of  $g(\alpha)/(0.5)$  are equivalent when an appropriate reaction model is used. Hence, it

can be concluded from Figure 5 that the best fit reaction model  $g(\alpha)$  for describing the thermal degradation process for PBAT/S blends is the reaction model R2, where

$$g(\alpha) = [1 - (1 - \alpha)^{1/2}] \quad (11)$$

### Determination of logarithm apparent pre-exponent factor

The logarithm apparent pre-exponent factor ( $\ln A_\alpha$ ) can be determined from the intercept of the straight line in Figure 3. By substituting the values of  $E_\alpha$  from Table 3, and the values of  $g(\alpha)$  from Equation 11 into the expression  $\ln [A_\alpha E_\alpha / Rg(\alpha)]$ ,  $\ln A_\alpha$  can be determined from the intercept of the line. The results are reported in Table 3. Figure 6 shows the variation of the logarithm pre-exponent factor as a function of conversion  $\alpha$ , which increased with increasing conversion  $\alpha$ . The logarithm apparent pre-exponent factor was  $30 \text{ min}^{-1}$  at  $\alpha = 0.1$  and increased rapidly to  $36 \text{ min}^{-1}$  at  $\alpha = 0.2$ , then increased slowly to  $39 \text{ min}^{-1}$  at  $\alpha = 0.9$ . The average value of logarithm apparent pre-exponent factor  $\overline{\ln A_\alpha}$  was  $37 \text{ min}^{-1}$ .

### CONCLUSION

Non-isothermal crystallization of biodegradable poly(butylene adipate-co-terephthalate)/starch blends was studied using differential scanning calorimetry from 25 to  $225^\circ\text{C}$  at four cooling rates of 5, 10, 15 and  $20 \text{ }^\circ\text{C} \cdot \text{min}^{-1}$ . A nitrogen atmosphere of  $20 \text{ mL} \cdot \text{min}^{-1}$  flowing rate was applied. There was only one crystallization peak in the exothermic experiment which shifted to a lower temperature as the cooling rate was increased.

The crystallization temperature varied from 98 to  $84^\circ\text{C}$  and the enthalpy varied from 11 to  $12 \text{ J} \cdot \text{g}^{-1}$  as the cooling rate was varied from 5 to  $20 \text{ }^\circ\text{C} \cdot \text{min}^{-1}$ ; the crystallization temperature decreased, but the crystallization enthalpy increased with an increasing cooling rate. The relative crystallinity as a function of time showed

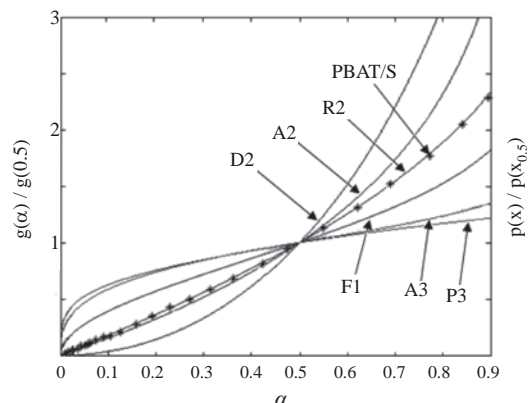


**Figure 5** Master plots of experimental data for  $p(x)/p(x_{0.5})$  and some theoretical reaction models  $g(\alpha)/(0.5)$  versus  $\alpha$  for poly(butylene adipate-co-terephthalate)/starch blends.

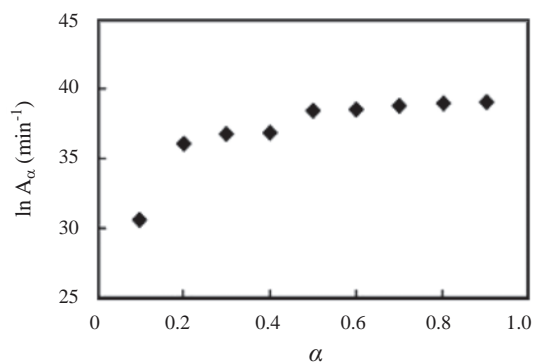


**Figure 6** Dependence of logarithm pre-exponent factor ( $\ln A_\alpha$ ) on conversion  $\alpha$  for poly(butylene adipate-co-terephthalate)/starch blends.

a longer crystallization time at a lower cooling rate. The crystallinity half time decreased with an increasing cooling rate (variation from 4 min to 2 min), which resulted in a shorter crystallization half time at a higher cooling rate.

Thermal degradation of the PBAT/S blends was studied using thermogravimetric analysis from 100 to  $800^\circ\text{C}$ , at five heating rates of 1, 2, 5, 10 and  $15 \text{ }^\circ\text{C} \cdot \text{min}^{-1}$ . The TGA curves showed two thermal degradation weight

loss stages. The derivative weight loss curves determined from the TG curves showed two peaks for each heating rate. The lower peak temperature occurred at 309–342 °C, as the heating rate was varied from 1 to 15 °C·min<sup>-1</sup> and was due to the degradation of the corn starch, while the higher peak temperature occurred at 375–420 °C as the heating rate was varied from 1 to 15 °C·min<sup>-1</sup> and was due to the degradation of PBAT.

The thermal degradation kinetic parameters were determined from the isoconversion Flynn-Wall-Ozawa model-free method. Both the apparent activation energy and the logarithm apparent pre-exponent factor increased with increased conversion  $\alpha$ . The average apparent activation energy and the average logarithm apparent pre-exponent factor for  $\alpha = 0.1 - 0.9$  were 266 kJ·mol<sup>-1</sup> and 37 min<sup>-1</sup>, respectively.

The reaction model  $g(\alpha)$  determined from the master plot method for PBAT/S was a phase-boundary controlled reaction, where  $g(\alpha) = [1 - (1 - \alpha)^{1/2}]$ .

### ACKNOWLEDGEMENT

This work was financially supported by the Kasetsart University Research and Development Institute (KURDI).

### LITERATURE CITED

Chiangga, S., S. Suwannasopon and N. Trivijitkasem. 2012. Thermal degradation of biodegradable poly(butylene adipate-co-terephthalate)/starch blends. **Kasetsart J. (Nat. Sci.)** 46: 653–661.

Chrissafis, K., K.M. Paraskevopoulos and D.N. Bikaris. 2006. Thermal degradation kinetics of the biodegradable aliphatic polyester, poly(propylene succinate). **Polym. Degrad. Stab.** 91:60–68.

Ge, X.C., Y. Xu, Y.Z. Meng and R.K.Y. Li. 2005. Thermal and mechanical properties of biodegradable composites poly(propylene carbonate) and starch–poly(methyl acrylate) graft copolymer. **Compos. Sci. Tech.** 65: 2219–2225.

Girija, B.G., R.R.N. Sailaja and G. Madras. 2005. Thermal degradation and mechanical properties of PET blends. **Polym. Degrad. Stab.** 90: 147–153.

Jankovic, B., B. Adnadevic and S. Mentus. 2007. The kinetic analysis of non-isothermal nickel oxide reduction in hydrogen atmosphere using the invariant kinetic parameters method. **Thermochim. Acta.** 456: 48–55.

Jun, C.L. 2000. Reactive blending of biodegradable polymers: PLA and starch. **J. Polym. Environ.** 8: 33–37.

Mano, J.F., D. Koniarova and R.L. Reis. 2003. Thermal properties of thermoplastic starch/synthetic polymer blends with potential biomedical applicability. **J. Mater. Sci. : Mater. Medicine.** 14: 127–135.

Mohanty, S. and S.K. Nayak. 2010. Aromatic-aliphatic poly(butylene adipate-co-terephthalate) bionanocomposite: Influence of organic modification on structure and properties. **Polym. Composites.** 31: 1194–1204.

Ramis, X., A. Cadenato, J.M. Salla, J.M. Moráncho, A. Valles, L. Contat and A. Ribes. 2004. Thermal degradation of polypropylene/starch-based materials with enhanced biodegradability. **Polym. Degrad. Stab.** 86: 483–491.

Saha, B. and A.K. Ghoshal. 2007. Model-free kinetics analysis of decomposition of polypropylene over Al-MCM-41. **Thermochim. Acta.** 460: 77–84.

Sanchez, M.E., M. Otero, X. Gomez and A. Moran, 2009. Thermogravimetric kinetic analysis of the combustion of biowastes. **Renew. Energ.** 34: 1622–1627.

Sugish, A.K. 2008. **Synthesis and Properties of Starch Based Biomaterials.** Ph.D.

dissertations. University of Groningen. Groningen, Netherlands.

Trivijitkasem, S., T. Sukkamart and P. Kadrun. 2008. Differential scanning calorimetric studies of non-isothermal crystallization of HDPE and HDPE/CaCO<sub>3</sub> composites. **Kasetsart J. (Nat. Sci.)** 42(4):776–783.

Vroman, I. and L. Tighzert. 2009. Biodegradable polymers. **Materials** 2: 307–334.

Vyazovkin, S. and C.A. Wight. 1999. Model-free and model fitting approaches to kinetic analysis of isothermal and nonisothermal data. **Thermochim. Acta**. 340–341: 53–68.